SANDIA REPORT

Simultaneous Time and Frequency Resolved Fluorescence Microscopy of Single Molecules

A. Khai Luong, Claudiu C. Gradinaru, David W. Chandler, Carl C. Hayden

Sandia National Laboratories

Simultaneous Time and Frequency Resolved Fluorescence Microscopy of Single Molecules

A. Khai Luong

Claudiu C. Gradinaru

David W. Chandler

Carl C. Hayden

Combustion Chemistry Department

Sandia National Laboratories
P.O. Box 9696, M.S. 9051
Livermore, CA 94450, U.S.A.

Abstract

Single molecule fluorophores were studied for the first time with a new confocal fluorescence microscope that allows the wavelength and emission time to be simultaneously measured with single molecule sensitivity. In this apparatus, the photons collected from the sample are imaged through a dispersive optical system onto a time and position sensitive detector. This detector records the wavelength and emission time of each detected photon relative to an excitation laser pulse. A histogram of many events for any selected spatial region or time interval can generate a full fluorescence spectrum and correlated decay plot for the given selection. At the single molecule level, this approach makes entirely new types of temporal and spectral correlation spectroscopy of possible. This report presents the results of simultaneous time- and frequency-resolved fluorescence measurements of single rhodamine 6G (R6G), tetramethylrhodamine (TMR), and Cy3 embedded in thin films of polymethylmethacrylate (PMMA).

Introduction and Background:

Single molecule fluorescence microscopy is a sensitive probe of the nano-environment surrounding the fluorescing molecule. Various fluorescence characteristics, such as the fluorescence intensity, spectrum, lifetime, and polarization, have been exploited to gain insights into the system under study.(1) These measurements on single molecules provide direct probes of the heterogeneity of a sample and the local environments within it, and with the appropriate time scale and resolution, reveal insights into the dynamics of the system. Single molecule experiments can be used to access photodynamics such as those involving transient states or energy transfer, and molecular or host dynamics that affect fluorescence characteristics.(2-5) The observation of individual molecules allows measurement of the distribution of dynamical processes that may be inherently averaged in ensemble measurements

Many sensitive, powerful techniques for measurements of fluorescence from single molecules have been developed based on various forms of time-resolved single-photon counting. Time-correlated single-photon counting (TCSPC) with fast-pulsed lasers provides measurements of fluorescence lifetimes with excellent time resolution. (6-9) Furthermore, continuous recording of absolute photon arrival times (time stamping) has become a powerful technique for studying fluorescence fluctuations with high temporal resolution.(10-12) The rate of photon arrivals provides a time trace of fluorescence intensity that can be used to study dynamics of the fluorescent system over a wide range of time scales. Both absolute arrival times and emission times relative to a pulsed laser can be simultaneously recorded to study, for example, fluorescence lifetime fluctuations.

By simultaneously probing multiple parameters of the fluorescent sample, one can further characterize the single molecule system. In particular, some of the motivations for developing single molecule multi-parameter measurements are: 1) to accurately identify multiple fluorophores within a single sample based on a range of fluorescence characteristics,(13) 2) to fully characterize the fluorescence of the molecule to obtain the most complete information on its local environment, 3) to gain insights into mechanisms that control the fluorescence properties by measuring auto and cross correlations of emission spectra, decay times, and intensities. The ability to measure these correlations is valuable for understanding both the fundamental photodynamics of the excited molecule and how the fluorescence reports on the local environment. Many factors determine the fluorescence characteristics, such as the local host environment, the orientation of the fluorophore relative to the excitation laser polarization, the internal electronic states of the fluorophore, and energy transfer from the excited fluorophore to a nearby acceptor fluorophore or quencher. Determining how these factors influence fluorescence-based measurements is important for the application of single molecule spectroscopy to probing local environments. For example, single-pair fluorescence resonance energy transfer (spFRET) is widely used as a sensitive ruler at the 2-10 Å scale in biological samples. Time-resolved multi-parameter measurements provide real time probes of these complex dynamics.

Several methods for multi-parameter fluorescence measurements of single molecules have been developed previously. Multi-wavelength fluorescence measurements with single molecule sensitivity have been achieved using multiple avalanche photodiode detectors (APD) and various filter schemes, providing fluorescence detection with high time resolution in two to four spectral windows.(13-17) This approach has been applied in particular for spFRET measurements.(14, 18, 19) The number of spectral windows is limited due to the increased

complexity of the experiment as the number of discrete APD detectors employed is increased. Many variations of this approach have been reported, including for example, a technique using two APDs to record the fluorescence intensity, lifetime and anisotropy.(20, 21) Techniques employing charge-coupled device (CCD) cameras have also been developed for single molecule multi-parameter fluorescence measurements. Using a CCD camera in conjunction with a dichroic wedge mirror and a Wollaston prism, simultaneous dual-color and dual-polarization measurements have been made.(22) Methods for recording full single molecule fluorescence spectra have also been developed using CCD cameras. (14, 23-25) However, CCD camera-based measurements are not single photon measurements, but integrate photons for a time interval, limiting their time resolution.

Several techniques to measure time- and wavelength-resolved fluorescence signatures with high resolutions in both parameter space have been reported for ensemble measurements.(26, 27, 28) We report here the initial results from a time- and frequency-resolved fluorescence microscope that permits the simultaneous measurement of the wavelength and emission time of every detected photon with single molecule sensitivity. The detection system relies on a commercially available multi-anode detector that is coupled to a home-built read out scheme that allows the simultaneous measurement of the arrival position and arrival time of every detected photon at photon rates exceeding one megaHertz. Our approach is inherently a TCSPC technique with the added capability to record the wavelength of each photon. We anticipate that this capability will be particularly advantageous to understanding the photophysical processes involved in spFRET measurements and to potentially making these measurements more quantitative. In addition, since this method records the arrival time and wavelength of each detected photon, the powerful statistical methods developed to analyze fluorescence fluctuations can now be applied to study spectral and lifetime correlations and fluctuations.

In this report, we will present initial results on time-and frequency-resolved fluorescence measurements of single rhodamine 6G (R6G), tetramethylrhodamine (TMR), and Cy3 molecules embedded in thin films of polymethylmethacrylate (PMMA). In the simplest demonstration, we use the technique to distinguish different fluorophores that have minimal differentiating fluorescence signatures in a sample environment. We also show results that demonstrate the more powerful capability of monitoring changes in multiple fluorescence characteristics of a sample as a function of time, providing new approaches to performing correlated fluorescence spectroscopy of single molecules.

Construction of New Microscope:

Schematically shown in Figure 1, the experiment couples a conventional confocal fluorescence microscope setup to a custom photon detection system. The excitation beam comes from a 50 MHz repetition rate, picosecond mode-locked laser (Time-Bandwidth Products) producing 532 nm laser light. It is expanded to fill the back aperture of a plan-apochromat 60X oil immersion objective (NA 1.40, Nikon) to produce an approximately diffraction limited spot size on the sample. The fluorescence emission is collected through the same objective. The excitation beam is made circularly polarized using a broadband $\lambda/4$ waveplate. Fluorescence passes through a 532 nm dichroic filter (Chroma Technology Corporation) and a 532 nm Raman edge filter (CVI Laser), and is confocally imaged through a 75 μm pinhole. Fluorescence coming through the pinhole is collimated, dispersed by an AR-coated SF14 prism (<3% loss for

5

both s/p polarizations, Optics For Research), and focused with a 75 cm cylindrical lens onto a position- and time-sensitive detector system. Sample scanning is accomplished with a piezoelectric-driven xy translation stage mounted on the inverted microscope (Nikon).
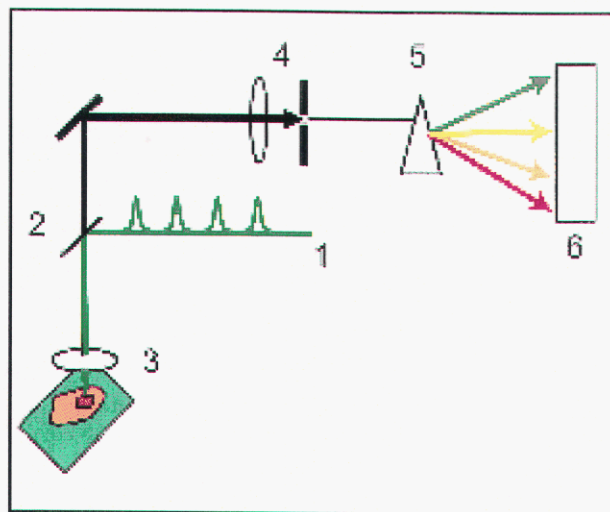
Figure 1: Schematic diagram of the experimental setup: 1) excitation laser, 2) dichroic filter, 3) objective, 4) imaging lenses and pinhole, 5) dispersing prism, and 6) time- and position-sensitive detector.

The time- and position-sensitive detection system is based on a commercially available multi-anode photomultiplier detector with 32 discrete elements (Hamamatsu Photonics, K.K.) coupled to custom read out electronics. The signals from the read out electronics are routed to constant fraction discriminators (CFD) and finally to time-to-digital converters (TDC). The timing electronics operate with the TDCs in the inverted mode so the start is provided by the detection of a photon and the stop is provided by the next laser shot. The digital information from the TDCs is transferred to a host computer. The read-out scheme simultaneously records the arrival anode position, hence the fluorescence wavelength, and the emission time relative to the excitation pulse for each detected photon. The overall data acquisition system can run at rates above one megahertz, well above the count rates encountered in single molecule fluorescence microscopy. The wavelength range and spectral resolution are determined by the dispersion and the imaging geometry. For the experiments reported here a full spectral range of 140 nm in the visible region is used. Due to the nonlinear dispersion of the prism, the spectral resolution is approximately 3 nm at 540 nm, and 5 nm at 650nm. The overall instrument time response function has a FWHM of about 300 ps; the electronics record photon emission times with a precision of 16 ps. The detector assembly is cooled to approximately 0°C, achieving a noise count of less than 10 Hz per anode element.

Sample Preparation for Single Molecule studies:

The samples were prepared by mixing the dyes in a solution of 4mg/mL of PMMA in toluene to give a dye concentration of 0.1nM. A small aliquot (50 μl) of this solution was deposited onto a clean glass coverslip and spincoated to form a thin layer of PMMA. The coverslips were cleaned by immersing them in a 12% HF/ethanol solution for 5 seconds, rinsing with nanopure water in two steps, and drying under nitrogen. The single molecule samples were

made with Cy3 only, R6G only, TMR only, and a mixture of R6G and TMR. Samples for bulk measurements of the dye fluorescence were prepared the same way but using a 1 μM dye concentration in the PMMA/toluene solution.

Images of the samples were recorded by raster scanning the sample with the piezoelectric stage. For the image data shown, a series of scans were taken of 5x5 μm^2 regions using 20 ms dwell time and 50 nm steps. Fluorescence time traces of individual molecules were also recorded. For the time traces, molecules were first located with a rapid raster scan of a 5x5 μm^2 using 10 ms dwell time and 100nm steps to avoid photobleaching the molecules. With the laser beam shuttered, the piezoelectric-driven stage was repositioned at the centroid of each cluster of bright pixels in the image corresponding to the location of a molecule. The shutter was then opened and data was acquired for 25 seconds with 10 ms time intervals. The laser was immediately shuttered at the end of each 25 second collection time. The data acquisition was repeated until irreversible photobleaching occurs.

Preliminary Results:

The distinguishing capability of this time- and frequency-resolved fluorescence microscope is the ability to *simultaneously* measure the fluorescence emission wavelength and time for every detected photon with single molecule sensitivity. By synchronizing the raster scan of the piezo-driven sample stage with the data acquisition, an image of the sample can be collected such that the fluorescence spectral and temporal information are simultaneously recorded for every detected photon in each pixel. Figure 2 shows a three-dimensional fluorescence intensity plot of a 5x5 μm^2 scanned region of a sample of mixed R6G and TMR dyes embedded in PMMA. The scan was taken with 50 nm pixels and 20 ms dwell time. This long dwell time and small pixel size was chosen to maximize the number of photons collected for each single molecule in a single scan. The region was scanned three consecutive times before a majority of the spots photobleached. To ensure that the intensity peaks in the image represent single molecule fluorophores the sample was made by spincoating a very dilute (0.1 nM) solution of dye. We also checked that the spatial FWHM of the peaks are equivalent to a diffraction limited spot, and confirmed that the peaks photobleached in a single step to the background level. The emission spectrum and decay trace for any pixel or clusters of pixels (appearing as a peak in the scanned image) can be generated by making histograms of the spectral and temporal data from every photon recorded in the selected pixel(s). To the right of the intensity map in Fig. 2 are the corresponding fluorescence spectra and decay plots for two selected single molecule peaks as indicated by the arrows. These results demonstrate that the detection system is capable of simultaneously measuring the fluorescence emission spectra and lifetimes from single molecules with a good signal to noise ratio. One use of these fluorescence signatures is to identify the corresponding fluorophores as discussed below.
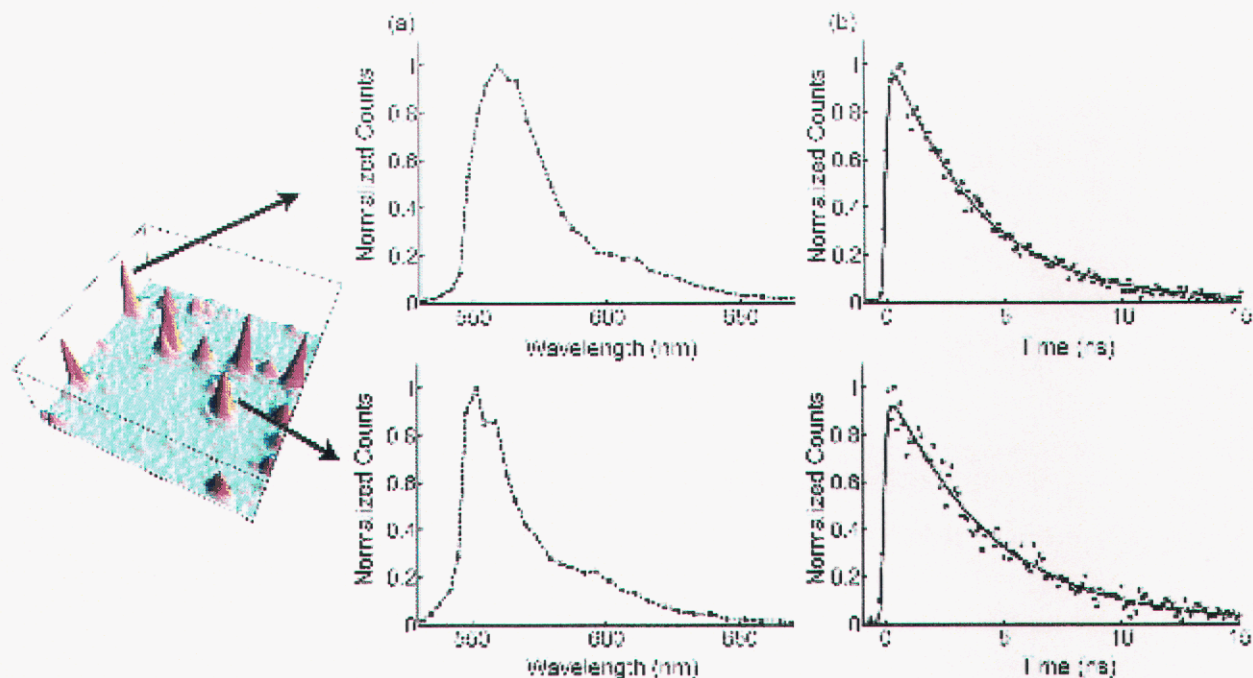
Figure 2: $5x5 \ \mu m^2$ region of a mixed sample of R6G and TMR embedded in a thin layer of PMMA. Column (a) shows the fluorescence spectra and column (b) show the fluorescence lifetimes of the selected peaks. Solid lines in the lifetime plots are the mono-exponential fits to the experimental data (open circles). Peak 1 lifetime $\tau_1 = 3.58$ ns, and peak wavelength = 559 nm. Peak 2 lifetime $\tau_2 = 4.14$ ns, and peak wavelength = 552 nm.

In order to differentiate between R6G and TMR molecules in the above image scan, the distribution of fluorescence characteristics for single molecules of R6G and TMR embedded in PMMA were separately determined first. The bulk spectrum and decay values are in good agreement with those found in the literature for bulk R6G and TMR in PMMA.(29, 30) The spectral peaks and lifetimes of the two dyes are different enough from each other to distinguish between R6G and TMR in bulk samples in PMMA. However, while the average values of the fluorescence characteristics from single molecules correspond well with the bulk values, the average fluorescence lifetime of TMR does not. Assuming the bulk measurement is representative of the sampled population mean, a statistical comparison to the mean of the single molecule measurements show a significant discrepancy between the two values. This discrepancy between the bulk and single molecule TMR measurements may arise from the effect of inhomogeneities in the polymer environment on the fluorescence characteristics of individual TMR molecules. While the twenty single molecule measurements sampled individual host sites, the bulk measurements sampled a much thicker volume of dye embedded PMMA material. Hence, the fluorescence lifetime is not a reliable parameter for discriminating between single R6G and TMR in the mixed single molecule sample.

Whereas the average fluorescence decay lifetimes are indistinguishable between the two single fluorophores, the simultaneously measured emission spectra of the two different dyes do provide means for discriminating between them. One simple approach is to consider the spectral peaks. The spectral peaks of single R6G molecules have a narrow distribution centered at 552

nm, while the spectral peaks for TMR molecules have a much broader distribution centered at 567 nm. Based on these characteristics, spot 1 in Figure 2 with emission peak at 559 nm can be assigned with high confidence to be a single TMR molecule because its spectral peak is outside the range observed for single molecule R6G. The emission spectrum for spot 2 peaks at 552 nm, which is the same value as the average peak wavelength for single molecule R6G in PMMA. However, due to the wide spectral variation of TMR in PMMA there is a small probability that this is a TMR molecule. With the simplifying assumption that the two distributions of spectral peaks are normal, we can assign a ~95% probability that the molecule at spot 2 is an R6G molecule. Clearly, more sophisticated methods for identification of fluorophores can be developed using the time- and frequency-resolved data, including methods based on the characteristics of individual photons. These results emphasize the importance of characterizing the behavior of the individual fluorophores in the sample environment before analyzing mixed samples. This is especially critical since it is common to observe large spectral variations in single molecule measurements(23, 31-33).

A unique capability of this time- and frequency-resolved fluorescence technique is the ability to simultaneously measure the fluorescence spectral and temporal information as a function of acquisition time for each detected photon. The data described below are examples of time- and frequency-resolved time trace measurements on single molecules of TMR and Cy3 in PMMA, and were chosen to illustrate the potential of the multi-parameter technique to probe fundamental photophysics in a correlated manner.
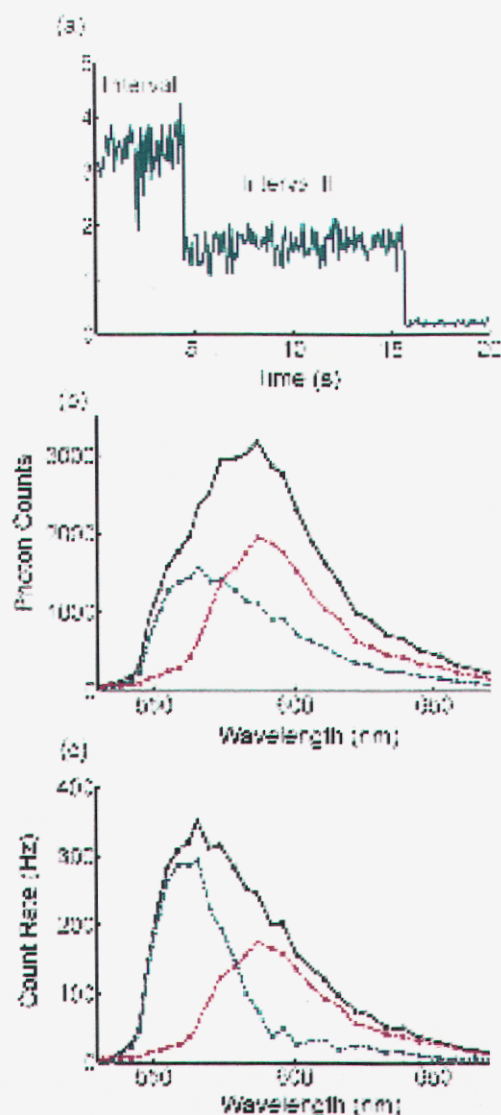
Figure 3: (a) Time trace of a diffraction limited spot of a sample of TMR embedded in PMMA film. (b) Fluorescence spectrum of the full time trace is shown by the black curve, the spectrum for the time Interval I is shown by the early rising curve, and the spectrum for the time Interval II is shown by the later rising curve. (c) Time-scaled fluorescence spectra for the time Intervals I and II are shown by the black and late rising curves, respectively. The blue curve is the difference spectrum between the two time-scaled fluorescence spectra.

Of fifty measurements taken on TMR, only twenty were found to have simple time traces with single step drops in intensity to the background level. The remainder of the time traces exhibit fluctuations not easily described by a single step photobleaching process. Figure 3a shows an example of such a time trace of a single diffraction limited spot of TMR in PMMA sample. The observation of two discrete intensity steps in a time trace ending at the background level, as seen in the figure, can be due to the sequential photobleaching of two molecules. The discrete step in the intensity level from a mean count rate of 3.36 kHz at early times to a lower level with a mean count rate of 1.65 kHz, and finally to background is a strong indication that there are two molecules. Thus, one would expect data from time interval I to yield a fluorescence signature with contributions from both molecules. These contributions are

10

independent if the molecules are not interacting. With one fluorophore photobleached, the emission spectrum from time interval II should only contain the signature of the single remaining fluorophore.

Because the emission wavelength and time relative to the excitation pulse are recorded simultaneously for each photon, we can select different time intervals of the time trace and histogram the fluorescence wavelengths and emission times of the photons arriving in that selected time region. This procedure results in a correlated fluorescence spectrum and lifetime surface for that time interval. The fluorescence spectra for the two selected intervals of the time trace is shown in Figure 3b. The fluorescence lifetime is almost the same in the two intervals with values of 3.90 ns and 3.70 ns for Intervals I and II, respectively. To examine whether or not there are two molecules emitting in Interval I, the emission spectra for the two intervals are scaled by the acquisition time of their respective intervals. The scaled spectrum from Interval II, where only one molecule is presumably emitting, is subtracted from the scaled total spectrum from Interval I where there may be two molecules emitting. These scaled spectra are shown in Figure 3c. The difference emission spectrum is typical of TMR in PMMA, and is due to the single fluorophore that was photobleached at the beginning of Interval II.

The analysis shown in Figure 3c is consistent with the notion that there were two non-interacting fluorophores with significantly different emission spectra in the focal volume. The fluorophore with the emission peak at 560 nm is photobleached first after 4.42 seconds of laser illumination, while the fluorophore with the emission peak at 590 nm, which is atypical for TMR, lives for 15.69 seconds. The drop from 3.36 kHz to 1.65 kHz count rate as one fluorophore photobleaches suggests that the two fluorophores had similar quantum yields at 532 nm excitation. A more definitive conclusion of the presence of two fluorophores in the focal volume, however, can be reached using anti-bunching techniques.(34)

While the results in Figure 3 illustrate the changes in fluorescence characteristics observed during the sequential photobleaching of two non-interacting fluorophores in the focal volume, Figure 4a shows a time trace that exhibits very different characteristics. This time trace was taken from a diffraction limited spot in a dilute (0.1 nM) sample of Cy3 embedded in PMMA in the same manner as were the R6G and TMR dyes. In this time trace plot the count rate is high, ~ 8.42 kHz, during Interval I, whereas the average count rate in Interval II is ~ 2.25 kHz, a factor of 3.7 lower. Interval I ends with a single step drop to the background count rate, followed by a dark period of nearly a second. Interval II starts with a single step rise after this dark period and ends 11 seconds later when the count rate again drops with a single step to the background level. The high count rate in interval I suggests there could be more than one molecule in the focal volume. However, the single step drop to the background level and the dark period is a strong indication that only one molecule was present, because it is highly improbable that all the molecules blinked into the off state simultaneously and remained synchronously off for nearly a second. Thus, it is concluded that the time trace of Figure 4a is taken from a single Cy3 molecule embedded in PMMA. Selecting the two different time intervals as indicated in the time trace plot, the fluorescence emission spectra and decay curves are generated and shown in Figure 4b-c, respectively.
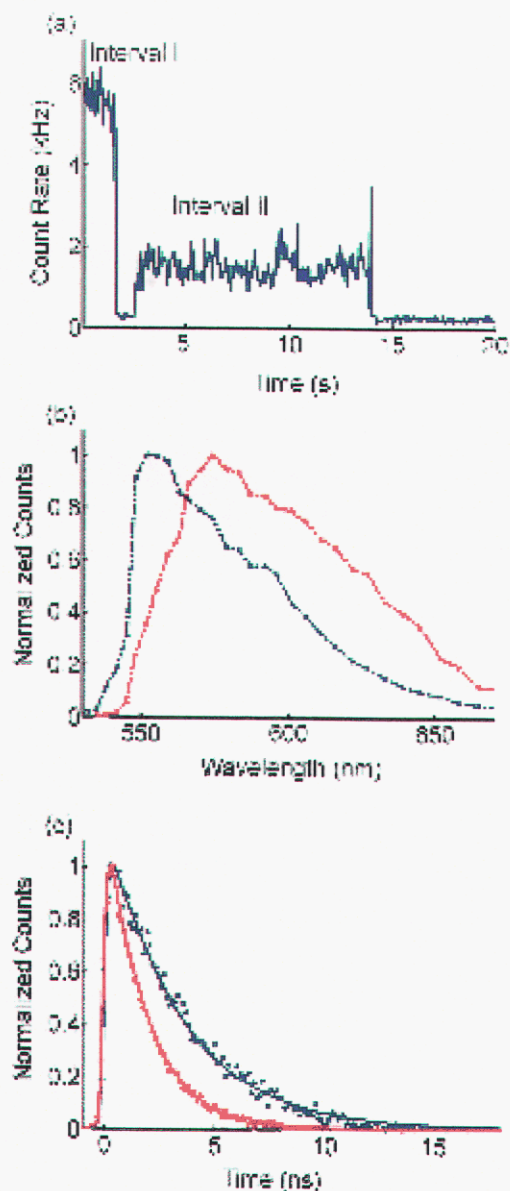
Figure 4: (a) Time trace of a diffraction limited spot in a sample of dilute Cy3 embedded in a thin layer of PMMA film. (b) Normalized fluorescence spectra of the time Intervals I and II are shown in two curves, with the spectrum peaking at higher wavelength coming from interval I. (c) The corresponding lifetime decays for the two time Intervals are shown to fit to mono-exponential curves: the longer decay curve corresponds to time Interval I and quicker decay curve to time Interval II.

Correlated with the large fluorescence intensity change, the fluorescence emission spectra and lifetimes of the single Cy3 embedded in PMMA also shifted significantly during the course of the time trace. The peak of the emission spectra shifted from 552 nm to 574 nm, with significant changes in the spectral shape. Simultaneously, the fluorescence lifetime dropped significantly from 3.30 ns to 1.70 ns. Thus, the red shift in the broad emission spectrum is correlated with a shift to shorter lifetimes. A possible explanation for this observed correlation is that there was a change in the interaction of the Cy3 with its host site that resulted in faster non-radiative relaxation of the dye molecule. This dynamic change caused the simultaneous red

shifting of the emission spectrum and reduction of the overall fluorescence lifetime and quantum yield.

The observations above for an example single Cy3 in PMMA is in sharp contrast to the static fluorescence characteristics observed for single Cy3 in PMMA, as shown by a few examples in Figure 5a-b. The single Cy3 molecules in PMMA exhibited wide spectral and temporal variations from molecule to molecule. However, there is a general trend that spectral peaks toward the red are correlated with longer fluorescence lifetimes, opposite from that observed in Figure 4. This correlation of spectrum and lifetime for individual single molecules may be due to differences in the energy level of the fluorescing electronic state in different host sites. A lower energy of the fluorescing state of the dye molecule will result in a more red-shifted spectrum and also slower non-radiative transitions, hence a lifetime that is longer.
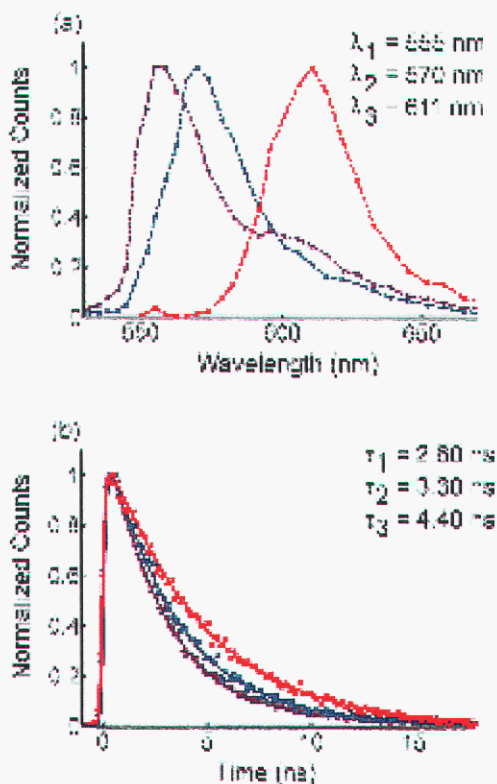
Figure 5: Shown are the fluorescence (a) spectra and (b) lifetime decays for individual single Cy3 molecules embedded in a thin layer of PMMA film.

The examples presented here are to demonstrate the distinctive strength of a simultaneous time- and frequency-resolved fluorescence microscope to record spectral and temporal fluctuations of fluorophore characteristics in a correlated manner, one photon at a time. A thorough examination of the photophysics behind these examples requires an analysis of many single molecule time traces and various controlled host environments, which is not the intent of this report.

Conclusions:

The correlations of the fluorescence intensity, wavelength, and emission time observed in these experiments were made possible by the simultaneous measurement of the fluorescence wavelength and emission time for each single detected photon. It is shown that these measurements can be made at the single molecule level, providing entirely new ways of performing single molecule correlation spectroscopy. The technique can be used to identify different fluorophores within a sample if the fluorescence characteristics of the individual fluorophores are well characterized under similar experimental conditions. This is critical for identification of single molecule fluorophores because of the ubiquitous fluctuating behavior observed under single molecule conditions. However, the time and frequency resolved microscope is best suited as a new tool for studying the fundamental dynamics underlying the photophysics of single molecules, such as changes in internal states of a single molecule, quenching, and resonance energy transfer processes. Experiments on single pair fluorescence resonance energy transfer in conjunction with development of correlation techniques that take advantage of the multi-correlated information are underway in our laboratory.

References:

1. Michalet, X., Kapanidis, A. N., Laurence, T., Pinaud, F., Doose, S., Pflughoefft, M. & Weiss, S. (2003) *Annu. Rev. Biophys. Biomol. Struct.* **32**, 161-182.
2. Xie, X. S. & Trautman, J. K. (1998) *Annu. Rev. Phys. Chem.* **49**, 441-480.
3. Moerner, W. E. (2002) *J. Phys. Chem. B* **106**, 910-927.
4. Moerner, W. E. & Fromm, D. P. (2003) *Rev. Sci. Instrum.* **74**, 3597-3619.
5. Nie, S. & Zare, R. N. (1997) *Annu. Rev. Biophys. Biomol. Struct.* **26**, 567-596.
6. Becker, W., Hickl, H., Zander, C., Drexhage, K. H., Sauer, M., Siebert, S. & Wolfrum, J. (1999) *Rev. Sci. Instrum.* **70**, 1835-1841.
7. Li, L.-Q. & Davis, L. M. (1993) *Rev. Sci. Instrum.* **64**, 1524-1529.
8. Minami, T., Kawahigashi, M., Sakai, Y., Shimamoto, K. & Hirayama, S. (1986) *J. Lumin.* **35**, 247-253.
9. Wilkerson, C. W., Goodwin, P. M., Ambrose, W. P., Martin, J. C. & Keller, R. A. (1993) *Appl. Phys. Lett* **62**, 2030-2032.
10. Yang, H. & Xie, X. S. (2002) *J. Chem. Phys.* **117**, 10965-10979.
11. Xie, X. S. (2002) *J. Chem. Phys.* **117**, 11204-11032.
12. Watkins, L. P. & Yang, H. (2004) *Biophys. J.* **86**, 4015-4029.
13. Prummer, M., Hübner, C. G., Sick, B., Hecht, B., Renn, A. & Wild, U. P. (2000) *Anal. Chem.* **72**, 443-447.
14. Ha, T., Enderle, T., Ogletree, D. F., Chemla, D. S., Selvin, P. R. & Weiss, S. (1996) *Proc. Natl. Acad. Sci. USA* **93**, 6264-6268.
15. Ha, T., Enderle, T., Chemla, D. S., Selvin, P. R. & Weiss, S. (1997) *Chem. Phys. Lett.* **271**, 1-5.
16. Tinnefeld, P., Herten, D.-P. & Sauer, M. (2001) *J. Phys. Chem A* **105**, 7989-8003.
17. Sabanayagam, C. R., Eid, J. S. & Meller, A. (2004) *Appl. Phys. Lett* **84**, 1216-1218.
18. Kühnemuth, R. & Seidel, C. A. M. (2001) *Single Mol.* **2**, 251-254.
19. Hohng, S., Joo, C. & Ha, T. (2004) *Biophys. J.* **87**, 1328-1337.
20. Schaffer, J., Volkmer, A., Eggeling, C., Subramaniam, V., Striker, G. & Seidel, C. A. M. (1999) *J. Phys. Chem. A* **103**, 331-336.

21. Hernando, J., van der Schaaf, M., van Dijk, E. M. H. P., Sauer, M., Garcia-Parajo, M. F. & van Hulst, N. F. (2003) *J. Phys. Chem A* **107,** 43-52.
22. Cognet, L., Harms, G. S., Blab, G. A., Lommerse, P. H. M. & Schmidt, T. (2000) *Appl. Phys. Lett* **77,** 4052-4054.
23. Lu, H. P. & Xie, X. S. (1997) *Nature* **385,** 143-146.
24. Weston, K. D. & Burrato, S. K. (1998) *J. Phys. Chem. A* **102,** 3635-3638.
25. English, D. S., Harbron, E. J. & Barbara, P. F. (2001) *J. Chem. Phys.* **114,** 10479-10485.
26. Courtney, S. H. & Wilson, W. L. (1991) *Rev. Sci. Instrum.* **62,** 2100-2104.
27. Kelly, L. A., Trunk, J. G. & Sutherland, J. C. (1997) *Rev. Sci. Instrum.* **68,** 2279-2286.
28. Tramier, M., Gautier, I., Piolot, T., Ravalet, S., Kemnitz, K., Coppey, J., Durieux, C., Mignotte, V. & Coppey-Moisan, M. (2002) *Biophys. J.* **83,** 3570-3577.
29. Deshpande, A. V. & Namdas, E. B. (2000) *J. Lumin.* **91,** 25-31.
30. Lee, M., Tang, J. & Hochstrasser, R. M. (2001) *Chem. Phys. Lett.* **344,** 501-508.
31. Geva, E., Reilly, P. D. & Skinner, J. L. (1996) *Acc. Chem. Res.* **29,** 579-584.
32. Novotny, L. (1996) *Appl. Phys. Lett* **69,** 3806-3808.
33. Wazawa, T., Ishii, Y., Funatsu, T. & Yanagida, T. (2000) *Biophys. J.* **78,** 1561-1569.
34. Basché, T., Moerner, W. E., Orrit, M. & Talon, H. (1992) *Phy. Rev. Lett.* **69,** 1516-1519.

Distribution

1	MS9055	Carl Hayden
1	MS9055	A. Khai Luong
1	MS9055	Claudiu Gradinaru
1	MS9054	David Chandler
1	MS9054	Bob Carling
1	MS9055	Andrew McIlroy
3	MS 9018	Central Technical Files, 8945-1
1	MS 0323	D. Chavez, LDRD Office, 1011
1	MS 0899	Technical Library, 9616
1	MS 9021	Classification Office, 8511/Technical Library, MS 0899, 9616 DOE/OSTI via URL